

Available online at www.sciencedirect.com**ScienceDirect**

Procedia Engineering 130 (2015) 1535 – 1543

**Procedia
Engineering**www.elsevier.com/locate/procedia14th International Conference on Pressure Vessel Technology

Study on Limit Loads for Safe End of Nuclear Pressure Vessel with Local Wall Thinning

J. Li^a, P. Cui^a, G.D. Zhang^b, F. Xue^b, C.Y. Zhou^{a,*}^a*School of Mechanical and Power Engineering, Nanjing Tech University, Nanjing, 211816, China*^b*Suzhou Nuclear Power Research Institute, Suzhou, 215004, China*

Abstract

Dissimilar metal welded joints are used in primary water systems of pressurized water reactor in nuclear power plant. They are mainly used to connect the ferritic steel pipe-nozzles of the pressure vessels such as reactor pressure vessels, steam generators and pressurizers with the austenitic stainless steel safe end. Thus, maintaining integrity of such joints is critical to ensure their safe service. As local wall thinning may probably appear at safe end due to erosion and corrosion, assessment methods with local wall thinning are urgently needed. In this paper, three-dimensional finite element analysis models with and without considering local wall thinning were built for dissimilar metal welded joints connected the safe end to pipe-nozzle of the reactor pressure vessel. A detailed analysis has been carried out to the limit load research of this structure. Results show that the bending load is the main factor influencing the stress distribution change and limit load. According to finite element results, the depth of local wall thinning should be the most important factor influencing limit load solution, while circumferential local wall thinning shows very small variation. Based on the finite element results prediction equations of limit loads for safe end with local wall thinning have been proposed.

© 2015 The Authors. Published by Elsevier Ltd. This is an open access article under the CC BY-NC-ND license (<http://creativecommons.org/licenses/by-nc-nd/4.0/>).

Peer-review under responsibility of the organizing committee of ICPVT-14

Keywords: local wall thinning, safe end of nuclear reactor, limit load, finite element

* Corresponding author. Tel.: +86-25-58139951; fax: +86-25-58139951

E-mail address: changyu_zhou@163.com

1. Introduction

The dissimilar metal welded joint of nuclear reactor pressure vesselsafe-ends is a special welding structure, relates to the primary loop of reactor pressure boundary, and is the key component of nuclear reactor. The dissimilar metal is usually used as a filler metal for pressure vessel nozzle for safe-ends. Because of the demand for design and application, it is difficult to manufacture this type of joints and welding for the dissimilar metal may induce defects. Meanwhile, due to complex welding thermal cycle, welded joints usually have the characteristic of low toughness, high welding residual stress, and corrosion fatigue cracking in service [1-4]. In addition, due to erosion and corrosion, the structure of safe-end will cause pits and wall thinning resulted from local metal loosing. Recently, research for safe-end with defects mainly focuses on damage and fracture in welded joints [5-11]. There have been many published papers on the straight pipe of local wall thinning defects, and the defect assessment methods have been reported in the API579 [12] and GB/T19624 [13]. However, due to structure itself, material and mechanical properties, the assessment methods for straight pipe would be not useful. So the research for limit load of safe-end with local wall thinning defects is necessary.

2. Finite element calculation

2.1. Structures and materials

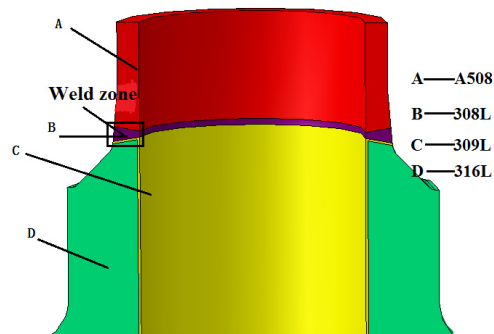


Fig. 1. Schematic illustrations of a typical safe end for dissimilar metal weld joint.

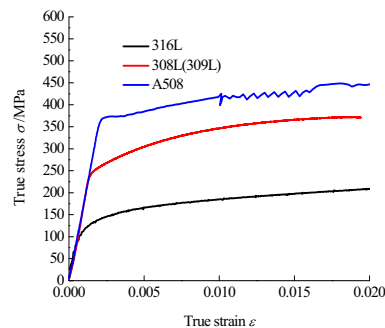


Fig. 2. The true stress-strain curves of four metal alloys at 340°C.

Figure 1 is a typical description of nuclear reactor pressure vessels safe end and dissimilar metal welded zone. They are mainly used to connect the ferritic steel pipe-nozzles of the pressure vessels such as reactor pressure vessels, steam generators and pressurizers with the austenitic stainless steel safe end. Nickel-base alloy is usually used as a filler metal in this type of welded joint for its thermal expansion coefficient laying between those of ferritic steel and austenitic stainless steel. The alloy can also significantly retard the carbon diffusion from the ferritic base metal to the weld metal. The design pressure is 17MPa and the temperature range is 288-340°C. The whole joint contains 4 metal alloys which are A508, 308L, 309L and 316L.

Based on the uniaxial tensile test results of 4 different materials, the mechanical parameters for calculation are acquired: the elastic modulus E is 180000MPa, poisson's ratio μ is 0.3, the service temperature is 340°C and the stress-strain curves for 4 metal alloys are shown in Fig. 2. Among them, the material mechanics parameters of 308L and 309L are consistent.

2.2. Defect size

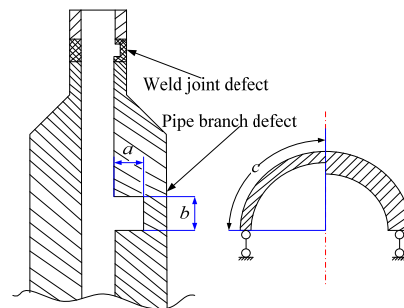


Fig. 3. The plane sketch of safe end with local wall thinning.

Table 1. Geometrical parameters.

No.	a/t	c/π
1#	0.2	0.2
2#	0.2	0.4
3#	0.2	0.6
4#	0.2	0.8
5#	0.2	1
6#	0.4	0.2
7#	0.4	0.4
8#	0.4	0.6
9#	0.4	0.8
10#	0.4	1
11#	0.6	0.2
12#	0.6	0.4
13#	0.6	0.6
14#	0.6	0.8
15#	0.6	1

The parameters for local wall thinning defects are depth a , axial length b , circumferential angle c and the specific sizes are as follows.

- (1) Depth $a/t=0.2, 0.4, 0.6$.
- (2) Axial length $b=a$.
- (3) Circumferential angle $c/\pi=0.2, 0.4, 0.6, 0.8, 1$.

Where t is the thickness of the wall. The plane sketch of safe end with local wall thinning is shown in Fig. 3. 15 finite element calculating models with different defect sizes are shown in Table 1. The local wall thinning defects would appear in 2 possible positions, one is located at welded joint and the other one is at pipe branch.

2.3. FE model

The commercial software ABAQUS is used to establish the finite element model. According to the symmetrical structure, 1/2 of actual structure is selected to establish the three-dimensional finite element model. The setting of boundary conditions and the corresponding load applied are shown in Fig. 4 (a), where the fixed constraint is in the right end of reactor pressure vessel, and the symmetry constraint is on the plane of symmetry. The internal pressure of pipes is 17MPa, and the equivalent axial load is applied on the left end of pressure vessel. The bending moment is applied on reference point of safe end in the right end by coupling method. C3D20R is chosen as element type of the model. With the changes of wall thinning size, the total number of mesh element varies in the range of 7593-11473 and the total number of corresponding nodes changes in the range of 36237-51168. The whole meshing model is shown in Fig. 4 (b) and Fig. 4(c).

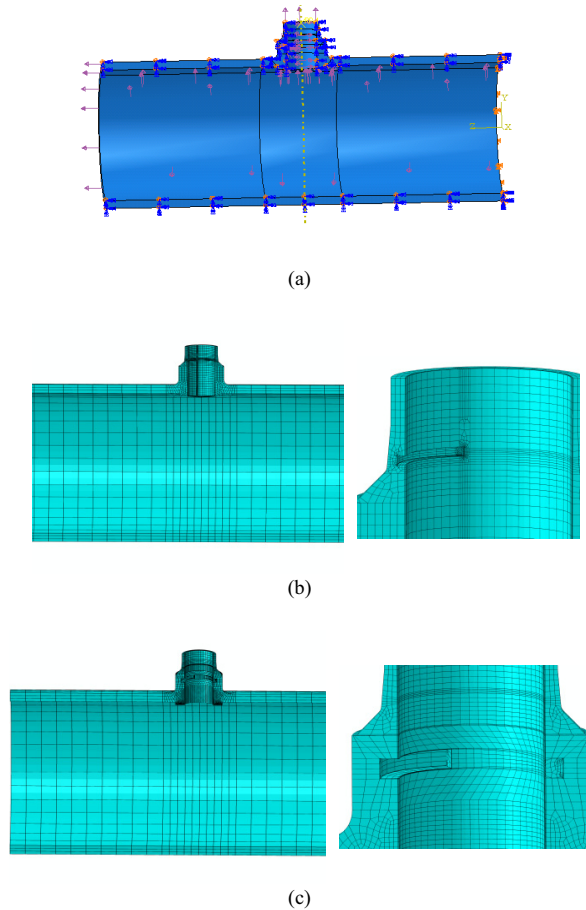


Fig. 4. FE boundary and mesh (a) Boundary (b) Mesh for safe end with weld joint defect (c) Mesh for safe end with pipe branch defect.

The limit load is obtained through twice elastic slope method, as shown in Fig. 5. In order to validate the independent of finite element mesh, 3 different mesh number models are compared and analyzed. The analysis results are shown in Fig. 5 and Table 2 showing that the mesh of study has no effect on results. When equivalent load $p \leq 1.0$, the structure is only subjected to internal pressure and the bending moment $M=0$. When equivalent load $p > 1.0$, the structure is subjected to internal pressure $P=17\text{MPa}$ and the bending moment $M=(p-1) \times 20000\text{MPa}$.

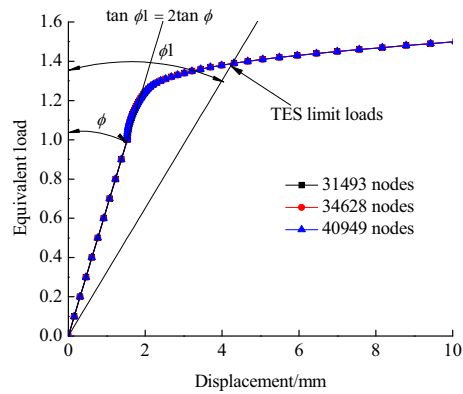


Fig. 5. Verification of the FE mesh precision.

Table 2. Verification of the FE mesh precision.

Nodes number	31493	34628	40949
Limit loads (KN·m)	7774	7774	7775

3. FE results for safe end with local wall thinning defects

3.1. Stress distribution in circumferential path for defect free safe end

Due to the obvious distinction of the results across circumferential path in the piping safe end part as the bending moment applies, for the convenience of analysis two paths are extracted to analyze in this section, one is at the welded joint and the other is at the pipe branch, shown in Fig. 6.

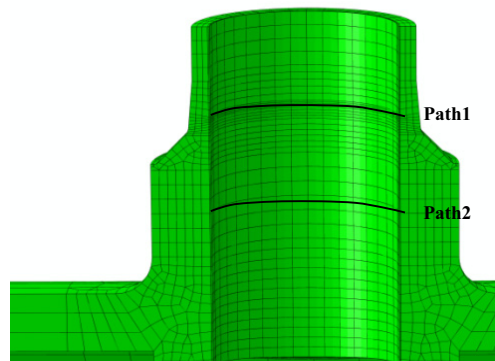


Fig. 6. Circumferential path.

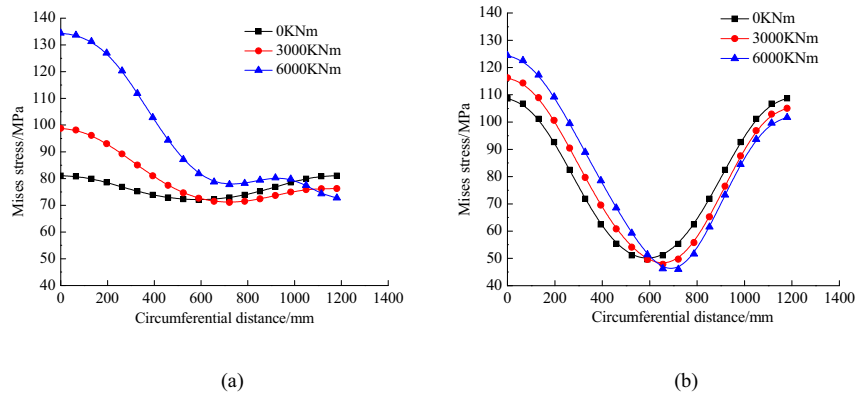
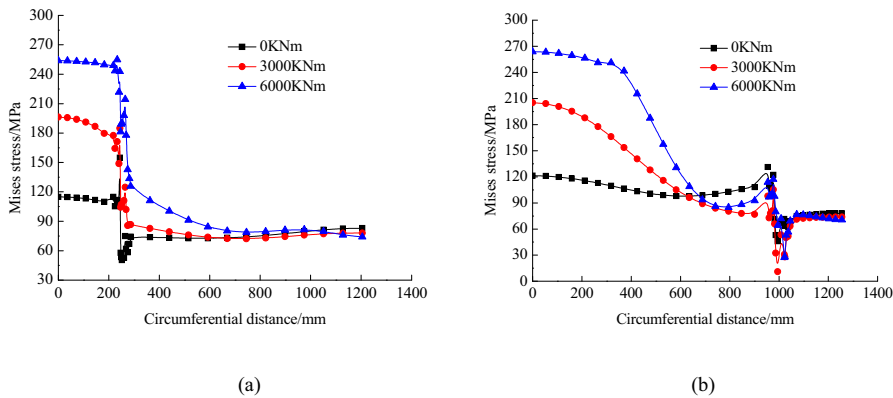


Fig. 7. Stress distribution in circumferential path for defect free safe end (a) Path1 (b) Path2.

Figure 7 is the stress distribution along circumferential path for defect free safe end. Results show that as the bending moment increases, stress varies apparently at the welded joint, while varies a little near pipe branch. When subjected to only inner pressure, stresses distribute evenly at the welded joint, and stress near pipe branch will firstly decrease and then increase. This is because of the influence of local stress concentration near pipe branch. As the applied bending moment increases, results change obviously in the tensile section at the left end of welded joints. It can be described that the change decreases along the path direction, while the change seems unobvious along the whole path near pipe bases.

3.2. Stress distribution in circumferential path for safe end with local wall thinning defects

The stress distribution in path1 and path2 of local wall thinning are shown in Figs. 8 and 9. According to stress distributions in these figures, results can be obtained as follows: Stress at local wall thinning section is wholly high, and increases with local wall thinning when the pure pressure is applied. This is due to the decreases of thickness. Stress rises sharply and then drops sharply, which is due to the stress distribution condition in discontinuous positions of components. For structures with local wall thinning, the effects of the increasing bending moment on stress distribution is very obvious. The tensile part at the left end of safe end is dangerous which is well worth investigation. Bending moment is the main load influencing limit load.



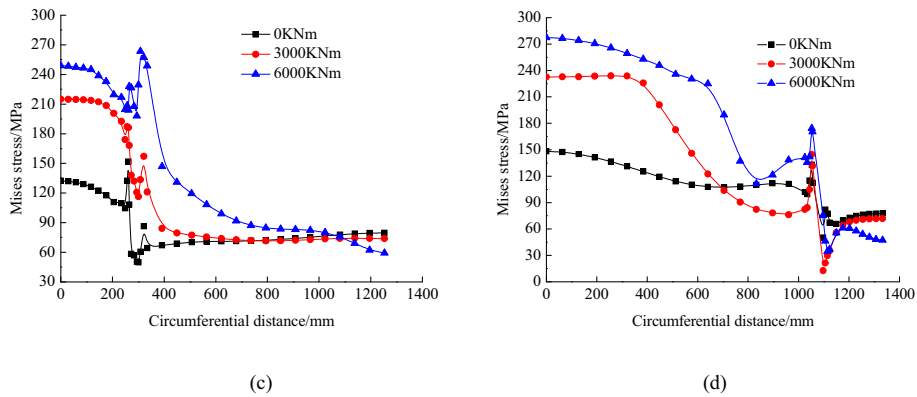


Fig. 8. Stress distribution in circumferential path for safe end with weld joint defects (a) $a/t=0.2$, $c/\pi=0.2$ (b) $a/t=0.2$, $c/\pi=0.8$ (c) $a/t=0.6$, $c/\pi=0.2$ (d) $a/t=0.6$, $c/\pi=0.8$.

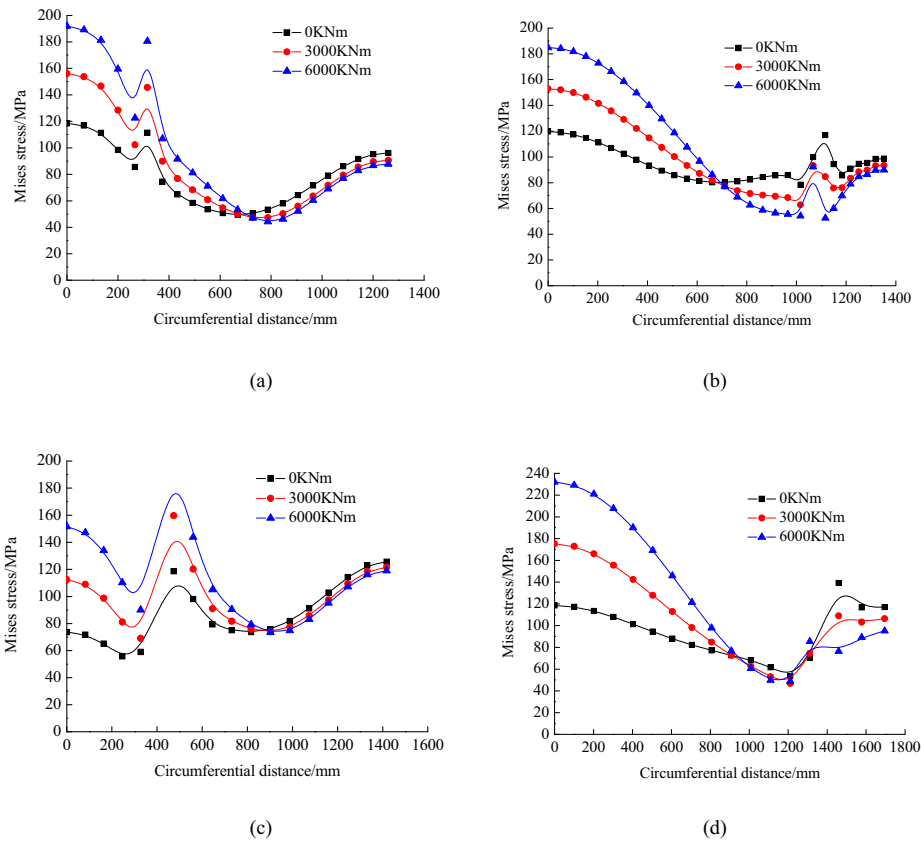


Fig. 9. Stress distribution in circumferential path for safe end with pipe branch defects (a) $a/t=0.2$, $c/\pi=0.2$ (b) $a/t=0.2$, $c/\pi=0.8$ (c) $a/t=0.6$, $c/\pi=0.2$ (d) $a/t=0.6$, $c/\pi=0.8$.

3.3. Limit loads for safe end with local wall thinning

Figure 10 depicts the results of limit load from FE calculation. The results show that, the limit load decreases with the size of defects increasing in general, and the limit load with defects is below those without defect. In addition, when local wall thinning depth is relatively shallow, the change of limit load with the thinning size increasing for the hoop direction is limited; when thinning depth is relatively larger, there are more significant influences on the limit load. Therefore, the thinning depth is the main factor affecting the limit load, and it should be paid particular attention to safe end.

Detailed comparison of the results shows that the limit load at welded joints is sensitive to the size of thinning defects. For example, for the same of thinning size, the limit load of welded joint is lower than that of pipe branch; the difference increases with increasing the depth of the thinning. The reason for the difference is the combined material's and structures discontinuousness at welded joint. In conclusion, size of thinning at weld should be paid attention, especially for thinning depth.

For the local wall thinning of welded joints, based on the FE results, the limit load of solution is proposed by fitting.

$$G = 0.7981 \cdot a^{-0.1315} \cdot c^{-0.02633} \quad (a=b) \quad (1)$$

where, $G=M_L/M_{L0}$, M_{L0} denotes the limit moment of safe end without defect, M_L denotes the limit moment of safe end with local wall thinning defect.

For the local wall thinning of the pipe branch, based on the FE results, the limit load of solution is proposed by fitting.

$$G = 0.9728 \cdot a^{-0.01524} \cdot c^{-0.005288} \quad (a=b) \quad (2)$$

The maximum error of regression is within $\pm 5\%$. The correlation coefficients are 0.925 and 0.947, respectively. This shows that the FE results are close to the predicted results.

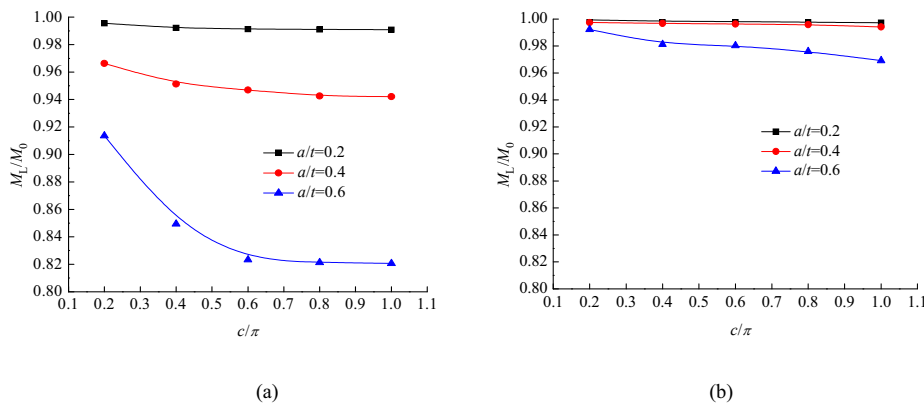


Fig. 10. Limit loads for safe end with different defect sizes (a) Weld joint defects (b) Pipe branch defects.

4. Conclusions

(1) The detailed research on stress distribution and limit load on safe end of dissimilar steel weld joint which has local wall thinning defects has been made. Results suggest that the bending load has particular significant effects on the stress distribution, and the safe end of dissimilar metal welded joints is a dangerous area. According to the limit

load results of finite element simulation, the circumferential thinning depth has little influence on the limit load, and the thinning depth is the major factor affecting the limit load.

(2) Limit load in the welded joints is more sensitive to thinning depth. The thinning depth on welds needs special attention in engineering application, especially the depth of thinning should be strictly controlled.

(3) Estimated solutions for safe end with local wall thinning are proposed according to finite element data which can be used to the safe assessment of safe end with local wall thinning.

References

- [1] M. Samal, K. Balani, M. Seidenfuss, An Experiment and Numerical Investigation of Fracture Resistance Behavior of a Dissimilar Metal Welded Joint, *Mech Eng Sci* 223 (2009) 1507-1522.
- [2] A. Chorin, Crack in Weld Area of Reactor Coolant System Hot Leg Piping at v. CIGC 2000-2823, 2000.
- [3] A. Jenssen, K. Norrgard, J. Lagerstron, Assessment of Cracking in Dissimilar Metal Welds. *Proceedings of 10th Int Symp. On Environmental Degradation of Materials in Nuclear Power Systems, Water Reactors, Minniapolis, USA, 2001*, pp. 231-243.
- [4] G. F. Li, G. J. Li, K. W. Fang, Stress Corrosion Cracking Behavior of Dissimilar Metal A508/52M/316L in Simulated PWR Primary Water Environment, *2th Int Symposium on Materials and Reliability in Nuclear Power Plants, Shenyang, China, 11-14 April 2011*.
- [5] Z. W. Liu, G. Z. Wang, F. Z. Xuan, C. J. Liu, S. T. Tu, Study on Failure Assessment Curves for Safe End of Nuclear Pressure Vessels, *Nuclear Power Engineering* 32 (2011) 169-172. (in Chinese)
- [6] M. Wei, G. Z. Wang, F. Z. Xuan, S. T. Tu, C. J. Liu, Leak-before-break analysis of a dissimilar metal welded overlay structure for connecting pipe-nozzle of nuclear reactor pressure vessel to safe end, *Nuclear Techniques* 37 (2014) 010603,1-5. (in Chinese)
- [7] N. Gong, G. Z. Wang, F. Z. Xuan, S. T. Tu, Leak-before-break analysis of a dissimilar metal welded joint for connecting pipe-nozzle in nuclear power plants, *Nuclear Engineering and Design* 255 (2013) 1-8.
- [8] L. Y. Du, G. Z. Wang, F. Z. Xuan, S. T. Tu, Effects of local mechanical and fracture properties on LBB behavior of a dissimilar metal welded joint in nuclear power plants, *Nuclear Engineering and Design* 265 (2013) 145-153.
- [9] H. T. Wang, G. Z. Wang, F. Z. Xuan, S. T. Tu, An experimental investigation of local fracture resistance and crack growth paths in a dissimilar metal welded joint, *Materials and Design* 44 (2013) 179-189.
- [10] H. T. Wang, G. Z. Wang, F. Z. Xuan, C. J. Liu, S. T. Tu, Local mechanical properties of a dissimilar metal welded joint in nuclear power systems, *Materials Science & Engineering A* 568 (2013) 108-117.
- [11] H. T. Wang, G. Z. Wang, F. Z. Xuan, S. T. Tu, Fracture mechanism of a dissimilar metal welded joint in nuclear power plant, *Engineering Failure Analysis* 28 (2013) 134-148.
- [12] API 579-1 ASME FFS-1-2007, Fitness- For-Service.
- [13] GB /T 19624-2004, Safety assessment for in-service pressure vessels containing defects. (in Chinese)
- [14] ASME, Rules for construction of nuclear facility components, New York, USA: ASME Boiler and Pressure Vessel Code Committee, Section III, NB. ASME, 2004.